Myosin VI is required for asymmetric segregation of cellular components during *C. elegans* spermatogenesis

Joseph F. Kelleher*†, Michael A. Mandell*, Gary Moulder‡, Katherine L. Hill§, Steven W. L'Hernault§, Robert Barstead‡ and Margaret A. Titus*

Background: The asymmetric division of cells and unequal allocation of cell contents is essential for correct development. This process of active segregation is poorly understood but in many instances has been shown to depend on the cytoskeleton. Motor proteins moving along actin filaments and microtubules are logical candidates to provide the motive force for asymmetric sorting of cell contents. The role of myosins in such processes has been suggested, but few examples of their involvement are known.

Results: Analysis of a *Caenorhabditis elegans* class VI myosin deletion mutant reveals a role for this motor protein in the segregation of cell components during spermatogenesis. Mutant spermatocytes cannot efficiently deliver mitochondria and endoplasmic reticulum/Golgi-derived fibrous-body membranous organelle complexes to budding spermatids, and fail to remove actin filaments and microtubules from the spermatids. The segregation defects are not due to a global sorting failure as nuclear inheritance is unaffected.

Conclusions: *C. elegans* myosin VI has an important role in the unequal partitioning of both organelles and cytoskeletal components, a novel role for this class of motor protein.

Addresses: *Department of Genetics, Cell Biology and Development, University of Minnesota, Minneapolis, Minnesota 55455, USA. ‡Department of Molecular and Cell Biology, Oklahoma Medical Research Foundation, Oklahoma City, Oklahoma 73104, USA. §Department of Biology, Emory University, Atlanta, Georgia 30322, USA.

†Present address: Exelixis Inc., 170 Harbor Way, South San Francisco, California 94083-0511, USA.

Correspondence: Margaret A. Titus
E-mail: titus@lenti.med.umn.edu

Received: 11 August 2000
Revised: 26 October 2000
Accepted: 27 October 2000

Published: 13 November 2000

Current Biology 2000, 10:1489–1496

0960-9822/00/$ – see front matter

Background

The cytoskeleton is involved in segregating cell contents, and actin-based motor proteins, in particular, have recently been found to have a role in several different types of partitioning. These include the asymmetric transport of RNA encoding a transcriptional repressor, Ash1p, in yeast [1–3], as well as the anchoring of components necessary for establishing embryonic and cell polarity in *C. elegans* and *Drosophila*, respectively [4,5]. Myosins comprise a diverse superfamily of actin-based motors defined by a conserved ATPase and actin-binding domain coupled to a divergent carboxy-terminal tail domain [6,7]. There are at least 15 distinct classes, as determined by phylogenetic analyses, each assigned a roman numeral on the basis of their order of discovery [7]. The class II myosins, which include skeletal muscle myosin II, are referred to as 'conventional' myosin as they are the best characterized. All others are collectively referred to as 'unconventional'. There are many classes of myosin, but there is a paucity of information about the roles of most of these classes during the sorting of cell contents that accompanies asymmetric cellular division.

Class VI myosin was recently shown to move toward the pointed end of actin filaments [8], a directionality distinct from all other characterized members of the myosin family, which move towards the barbed end. Thus, myosin VI may be involved in sorting cell components in a manner distinct from all other myosins. Current evidence suggests that it has roles both in particle transport and in pulling membranes down along polarized actin filaments [9,10].

Development of specialized cells, tissues and organs in the simple metazoan *C. elegans* provides many striking examples of unequal or asymmetric partitioning, and offers a chance of exploring the role of the cytoskeleton in these processes. Spermatogenesis is one interesting example of partitioning in *C. elegans* that previous work has shown to be amenable to genetic and cell biological analysis [11]. As in other metazoans, nematode spermatogenesis involves dramatic asymmetric partitioning of cellular contents as specific organelles, vesicles and cytoplasmic components are selectively sorted into developing sperm while other cellular contents are selectively excluded. The actin cytoskeleton has been implicated in segregation during spermatogenesis in *C. elegans*. Mutations in *spe-26*, which encodes a protein with homology to the actin-binding proteins kelch and scruin, show mis-segregation of chromosomes and cellular components during spermatogenesis [12]. It is not known whether active movement of organelles and developmental determinants during *C. elegans* spermatogenesis requires myosins. The ability to identify deletions in a gene of interest in *C. elegans* has resulted in the isolation of a class VI myosin mutant with a defect in spermatogenesis, and has uncovered a role for this motor protein in asymmetric segregation.

Results and discussion

A reverse genetic approach was used to investigate the roles of myosin motors in *C. elegans*. The *C. elegans* genome encodes eight unconventional myosins ([13], and J.F.K. and M.A.T., unpublished data), but particular functions have not been identified for any of these motor proteins. The first phenotypic characterization of any unconventional myosin in *C. elegans*, the myosin VI encoded by *hum-3* (heavy chain of unconventional myosin) [13], is reported here. HUM-3 is highly homologous to both *Drosophila* and mouse myosin VI [13] and contains a myosin VI-specific insertion of 50 amino acids in the converter domain that is believed to be responsible for the unique 'backwards' directionality of this myosin [8,13]. Animals bearing a 2.4 kb deletion within the *hum-3* gene on chromosome I were isolated from a population of chemically mutagenized animals using a PCR-based screen. Bases 394–2790 in cosmid F47G6 (GenBank accession number AF098989) are deleted in the resulting mutant, *ok153*, removing sequences that encode the core of the HUM-3 myosin VI motor domain (Figure 1a), including the nucleotide-binding site.

C. elegans has two sexes: self-fertile hermaphrodites that make both sperm and oocytes, and males that make only sperm. Mutant hermaphrodites homozygous for *hum-3*(*ok153*) have no apparent somatic defects but they contain defective sperm, which causes a Spe phenotype. Homozygous *hum-3(ok153)* mutant hermaphrodites are largely self-sterile, with 79% failing to produce any progeny and 21% producing a mean of only 2.5 progeny at 20°C (n = 92), whereas 97% of heterozygous *hum-3*(*ok153*)/+ siblings are completely fertile, producing over 100 progeny per animal (n = 193). Fertility was further reduced at 25°C, with 97.9% failing to produce any progeny and 2% producing one progeny (n = 49). Observation of self-sterile hermaphrodites by differential interference contrast (DIC) microscopy reveals that oocytes are produced in the gonad but they are not fertilized, despite the presence of sperm in the spermatheca. Mating *hum-3*(*ok153*) hermaphrodites to wild-type males results in normal broods of viable progeny (n = 50), therefore wild-type sperm can rescue all fertility defects in *hum-3*(*ok153*) hermaphrodites. Homozygous *hum-3(ok153)* males are sterile (99% sterile, n = 89), failing to produce cross progeny with genetically marked hermaphrodites that are wild-type at the *hum-3* locus. The tester hermaphrodites produced normal broods of self progeny, indicating that *hum-3*(*ok153*) male-derived sperm did not compete with the hermaphrodite-derived sperm.

Figure 1

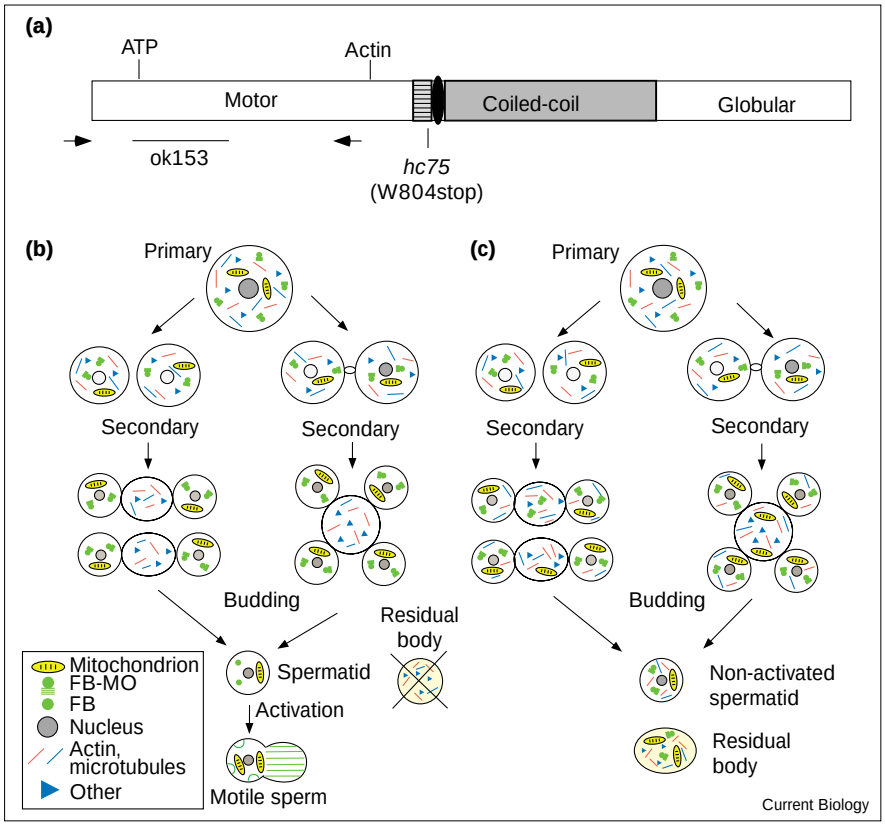

Mutations in *spe-15*(*ok153*) cause spermatogenesis defects in *C. elegans*. (a) Schematic diagram of HUM-3 predicted protein sequence. The position of the ATP- and actin-binding regions are indicated. The small horizontally striped box represents the region of the myosin VI head that contains a unique 50 amino acid insert at the base of the converter region, the oval represents the single light-chain-binding IQ region. The region deleted in *ok153* is denoted by the solid line. Arrows indicate the location of the internal primers used in the PCR screen. Also indicated is the position of the premature stop codon in *spe-15*(*hc75*) (W804stop). (b) Schematic diagram of morphological changes and asymmetric partitioning during spermatogenesis in wild-type *C. elegans*. Primary spermatocyte (top) divides to form two secondary spermatocytes that may (left) or may not (right) complete cytokinesis to give rise to the structures below. Spermatids bud from the residual body in both cases and, upon activation, polymerize major sperm protein (green hatching) and become motile spermatozoa. The residual body and its contents are ultimately degraded. Note that each spermatid would have many mitochondria and FB-MOs. The triangles indicating 'other' components represent ribosomes, Golgi and endoplasmic reticulum. (c) Schematic diagram of morphological changes and failed asymmetric partitioning during *spe-15*(*ok153*) spermatogenesis.

The genetic position of *hum-3* is close to three previously described Spe genes: *spe-8*, *spe-13* and *spe-15* [14]. *hum*-3(*ok153*) complements *spe-8*(*hc40*) and *spe-13*(*hc137*) but fails to complement *spe–15(hc75)* ($n = 59$ sterile *hum-3*(*ok153*)/*spe-15*(*hc75*) transheterozygous animals). For *spe-15*, complementation tests were performed reciprocally by crossing *hum-3*(*ok153*)/+ males to *spe–15*(*hc75*) hermaphrodites, and *spe-15*(*hc75*)/+ males to *hum-3* hermaphrodites, with the same result: *spe-15*(*hc75*)/*hum-3*(*ok153*) transheterozygotes are sterile. Two previously uncharacterized mutations conferring Spe phenotypes, *eb10* and *eb56*, map near *spe-15* and were recently shown by complementation analysis to be *spe-15* alleles (G. Zhu and S.W.L'H., unpublished observation). A molecular lesion resulting in a premature stop codon in the *hum-3* gene was found in *spe-15*(*hc75*) (Figure 1a) by sequencing the *hum-3* locus in DNA derived from this mutant. Therefore, *ok153* is an allele of *spe-15* and the strain will be hereafter referred to as *spe-15*(*ok153*).

The terminal stages of spermatogenesis in wild-type *C. elegans* involve extensive cellular changes and complete partitioning of cellular contents between developing spermatids and an acellular remnant, referred to as the residual body (RB) [11]. Meiotic division of each primary spermatocyte yields two *2N* secondary spermatocytes that sometimes undergo incomplete cytokinesis (Figure 1b) and so may remain attached [15]. During meiosis II, spermatids bud, leaving behind the RB [15]. As spermatids bud from the RB, organelles and cytosolic components are differentially segregated either into the spermatids or into the RB (Figure 1b). Spermatids inherit all the mitochondria, specialized structures called fibrous-body membranous organelles (FB-MOs) containing major sperm protein (MSP), and one centrosome and a haploid nucleus. Other cellular components, including most detectable actin and tubulin, are packaged into the RB and degraded [16].

The *spe-15*(*ok153*)mutant was used for a detailed phenotypic analysis as this deletion mutant is likely to be a null allele of *spe-15*. Spermatocytes derived from *spe-15*(*ok153*) mutant animals undergoing the process of spermatid budding show gross cytological defects suggestive of underlying sorting defects. The residual body, which appears smooth in wild-type spermatocytes (Figure 2a,b), appears pocked and vacuolated in *spe-15*(*ok153*) spermatocytes when observed by DIC microscopy (Figure 2c,d). This morphology is typical of mutants that have FB-MO defects [17,18]. Budding spermatids often appear multilobed and misshapen in *spe-15*(*ok153*) spermatocytes (Figure 2d), in contrast to wild-type spermatids, which are uniform and round as they bud (Figure 2a,b).

Labeling with markers for specific cellular components shows that *spe-15*(*ok153*) spermatocytes fail to partition certain organelles properly during spermatid budding. In wild-type spermatocytes, FB-MOs and mitochondria normally segregate completely into the budding spermatids and are excluded from the RB. In contrast, FB-MOs (Figure 3) and mitochondria (Figure 4) are present in the RB and in spermatids of *spe-15*(*ok153*) spermatocytes. The degree of mislocalization in *spe-15*(*ok153*) spermatocytes is variable: 66% of cells have a uniform distribution of FB-MOs in spermatids and throughout the entire RB, 23% of cells have MOs in spermatids and in regions of the RB immediately adjacent to the forming spermatid and 11% of cells appear to have a normal distribution, despite morphological defects such as misshapen or multilobed spermatids ($n = 65$). Mitochondria have a similarly variable distribution between spermatids and the RB in *spe-15*(*ok153*) spermatocytes, with some spermatocytes properly sorting mitochondria to spermatids despite defects in spermatid shape.

The *spe-15*(*ok153*) spermatids contain dramatic accumulations of actin filaments, in marked contrast to wild-type

Figure 2

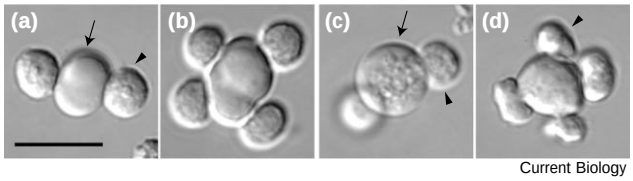

spe-15(*ok153*) spermatocyte morphology is aberrant. Differential interference contrast (DIC) micrographs of live (a,b) wild-type and (c,d) *spe-15(ok153)* secondary spermatocytes during budding of spermatids from the residual body (RB). Arrows point to the RB and the arrowheads to budding spermatids. Note the vesiculated appearance of the RB and irregular, multilobed appearance of budding spermatids in *spe-15*(*ok153*) spermatocytes. Scale bar represents 5 μm.

Figure 3

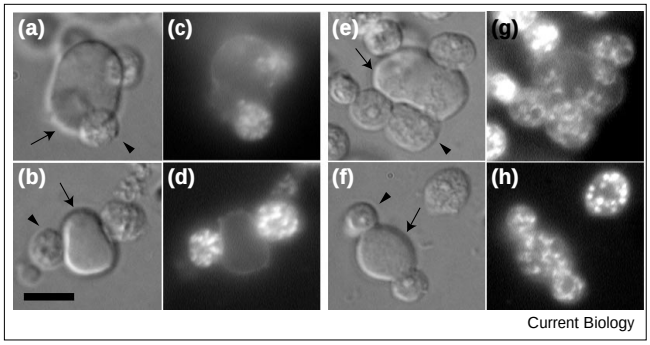

FB-MOs are not fully segregated into budding *spe-15*(*ok153*) spermatids. Live (a–d) wild-type and (e–h) *spe-15*(*ok153*) budding secondary spermatocytes stained with fluorescent wheat-germ agglutinin to visualize membranous organelles (MOs), visualized by (a,b,e,f) DIC and (c,d,g,h) fluorescence microscopy. Arrows point to the residual body and arrowheads to budding spermatids. Scale bar represents 5 μm.

Figure 4

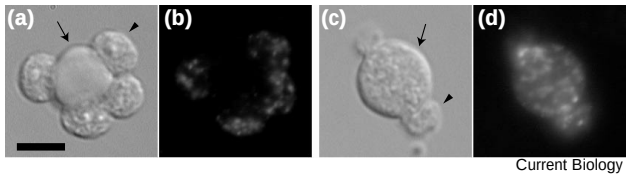

Mitochondria are not fully segregated into budding *spe-15*(*ok153*) spermatids. Live (a,b) wild-type and (c,d) *spe-15*(*ok153*) spermatocytes stained with COX1 antibody to visualize mitochondria. (a,c) DIC and (b,d) fluorescence micrographs. Arrows point to the residual body and arrowheads to budding spermatids. Scale bar represents 5 μm.

spermatids (Figure 5, compare b with d, f, and h) that completely lack actin filaments [16]. As with the organelle-sorting defects, the degree of accumulation of actin filaments varies among *spe-15*(*ok153*) spermatids (Figure 5d,f,h). Thirty-six percent of *spe-15*(*ok153*) spermatids labeled with phalloidin and imaged at random contain little or no actin, 30% have faint staining, often present in a cortical distribution, and 34% display intense staining, with aggregates of actin filaments throughout the spermatids (n = 171).

The failure to partition actin filaments correctly in *spe-15*(*ok153*) spermatocytes is not apparently due to gross defects in actin filament structure or arrangement during spermatid budding (Figure 6). The distribution of F-actin was analyzed during spermatid budding of wild-type spermatocytes and found to be restricted to the cortex of the developing RB (Figure 6d–f). There is an apparent concentration of F-actin at the region where the spermatid is budding (Figure 6d,e, arrows). Phalloidin also labels the cortex of budding *spe-15*(*ok153*) spermatocytes and has an apparent concentration at sites of budding (Figure 6h, arrows). Interestingly, there is no obvious actin staining in the *spe-15*(*ok153*) spermatids during budding. On the basis of the similar actin filament distribution in budding wild-type and mutant secondary spermatocytes, it is not yet clear why *spe-15*(*ok153*) spermatids contain actin filaments whereas wild-type spermatids lack them.

Interestingly, tubulin is also aberrantly sorted in *spe-15*(*ok153*) spermatocytes (Figure 7). Tubulin is normally sorted to and retained in the RB of wild-type spermatocytes ([19], and Figure 7a,b). In the *spe-15*(*ok153*) spermatocytes, however, tubulin is observed in the spermatids during budding (Figure 7c–f) and often appears to be accumulated near the plasma membrane. Isolated *spe-15*(*ok153*) spermatids also stain for tubulin (Figure 7k–n), whereas wild-type spermatids do not (Figure 7g–j). The tubulin distribution in budding spermatocytes is reminiscent of that observed in *spe-4* mutants which, although they fail to properly bud spermatids, also show accumulations of tubulin staining at the periphery of the spermatocyte [20]. SPE-4 is a presenilin protein family member required for the morphogenesis of FB-MOs and is also required for asymmetric partitioning of cellular components [20].

Not all aspects of partitioning into *spe-15*(*ok153*) spermatids fail. Nuclei are visible in more than 99% of *spe-15*(*ok153*) spermatids, both by DIC (n = 220) and Hoechst 33342 staining (n = 50). Thus, the *spe-15*(*ok153*) spermatocytes do not have a complete failure of the normal partitioning machinery, as indicated by the fact that in some cases MOs and mitochondria are normally distributed.

Organelle segregation is essential for the delivery of components necessary for spermatid activation and sperm function. Nematode spermatogenesis results in non-flagellated spermatozoa that use MSP-driven pseudopod extension for amoeboid motility [16]. Spermatids activate to motile spermatozoa *in vivo* upon mating and *in vitro* in response to a number of treatments [21]. Activation occurs as MOs fuse with the plasma membrane. Following this

Figure 5

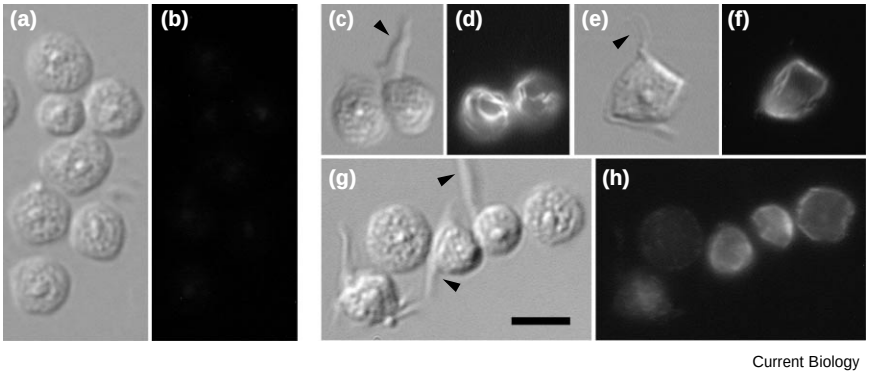

spe-15(*ok153*) spermatids contain F-actin. (a,b) Wild-type and (c–h) *spe-15*(*ok153*) spermatids fixed and labeled with fluorescent phalloidin to visualize actin filaments. (a,c,e,g) DIC and (b,d,f,h) fluorescence micrographs. Actin filaments are absent from wild-type spermatids but are present to varying degrees in *spe-15*(*ok153*) spermatids. Arrowheads in (c,e,g) indicate spike-like projections from *spe-15*(*ok153*) spermatids that do not label with phalloidin. Scale bar represents 5 μm.

Figure 6

Actin localization is normal in budding *spe-15*(*ok153*) spermatocytes. Paired DIC and fluorescent micrographs of fixed dividing (a–f) wild-type and (g,h) *spe-15*(*ok153*) secondary spermatocytes labeled with fluorescent phalloidin. Arrowheads highlight actin filaments concentrated at bud sites of forming spermatids. Scale bar represents 5 μm.

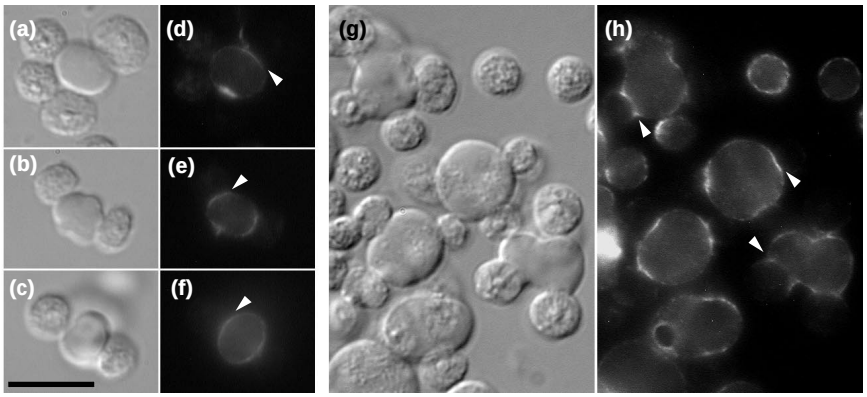

fusion and release of soluble MSP into the cytosol, a single pseudopod containing polymerized MSP is extended and the sperm moves [22].

Spermatids dissected from *spe-15*(*ok153*) mutant animals fail to activate *in vitro* (Figure 8, compare a and b with c–e). The majority of *spe-15*(*ok153*) spermatids remain either as rounded cells (48%) or display large, rod-like inclusions through the cell body after activation (36%). These inclusions do not label with phalloidin and are thus unlikely to be composed of actin. Similar rod-like structures are seen in other Spe mutants and are believed to contain polymerized MSP [15]. Other aberrant morphologies present in activator-treated *spe-15*(*ok153*) spermatids include multiple small spike-like projections (5%) (Figure 8e), an activation intermediate seen in wild-type sperm [23]. Only 1% of *spe-15*(*ok153*) spermatids activated *in vitro* develop a pseudopod. In comparison, 85% of wild-type spermatids display a well defined pseudopod (Figure 8a,b), with only 3% of cells remaining round and 1% containing inclusions. Thus, the incorrect sorting of cellular constituents is strongly correlated with a profound and severe defect in sperm function and is likely to prevent normal activation.

The phenotype of the *spe-15(ok153)* mutant reveals a novel role for myosin VI in asymmetric sorting of cellular components. The myosin VI encoded by *spe-15(hum-3)*

Figure 7

Budding *spe-15*(*ok153*) spermatids contain tubulin. DIC and fluorescence micrographs of budding spermatocytes and spermatids fixed and stained with a tubulin monoclonal antibody to visualize tubulin. Samples from (a,b,g–j) wild-type and (c–f,k–n) *spe-15*(*ok153*) worms are shown. Tubulin is present in the residual body but absent from budding spermatids in wild-type spermatocytes, but is present in both the *spe-15*(*ok153*) residual body and budding spermatids (c–f).The arrow in (e) indicates the nucleus in the budding spermatid.

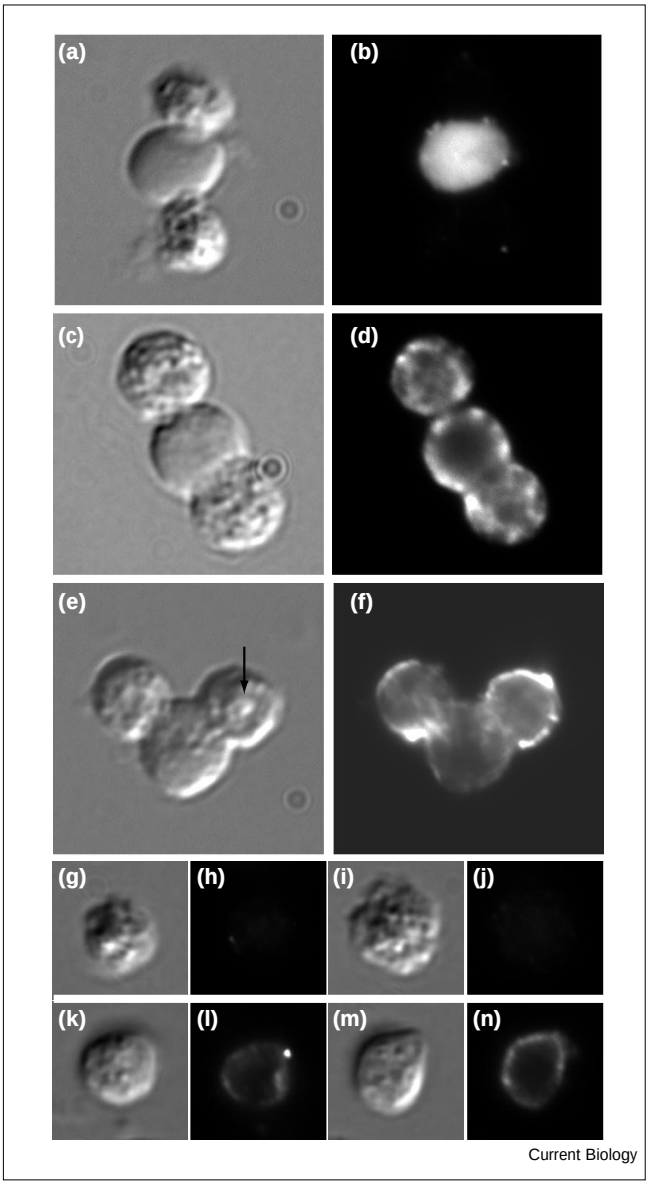

Figure 8

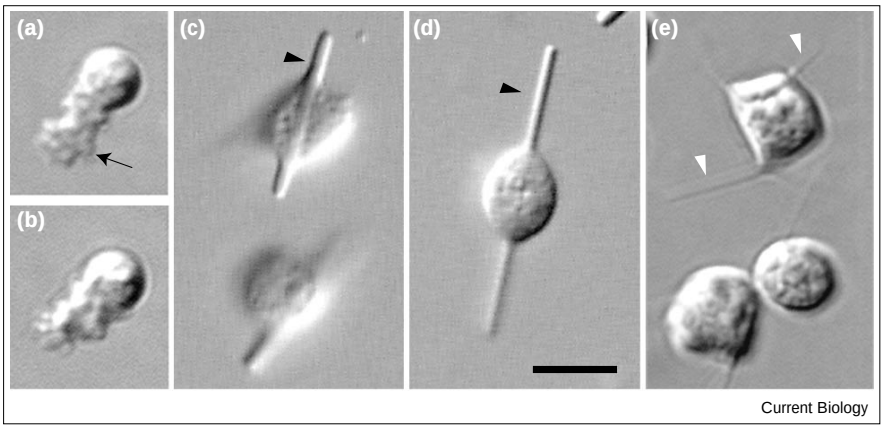

spe-15(*ok153*) spermatids have activation defects. DIC micrographs of spermatids activated *in vitro*. (a,b) Wild-type spermatozoa have a single large pseudopod (arrow). (c–e) Under identical conditions, *spe-15*(*ok153*) spermatids form large rod-like inclusions (black arrowheads) or multiple small spikes (white arrowheads) or remain round (data not shown). Scale bar represents 5 μm.

[13] is required for the proper and complete partitioning of mitochondria, FB-MOs, actin filaments and microtubules, but is not required for nuclear segregation or spermatid budding (Figure 1c). The partitioning defects are variable, indicating that other mechanisms of asymmetric sorting are operating in late spermatogenesis. The small proportion of *spe-15*(*ok153*) spermatids that are able to activate may not be functional if, because of sorting errors, they lack any of the components necessary for fertilization. The *spe-15*(*ok153*) phenotype suggests that myosin VI may either act directly as an organelle motor, trafficking mitochondria and FB-MOs to the budding spermatids, or that it might have a role in maintaining cytoskeletal elements and organelles in their appropriate compartments by organizing both actin and microtubules in the spermatocyte during the final stages of spermatid budding. The observation that both actin and microtubules are aberrantly segregated tends to support the hypothesis that myosin VI has a role in mediating or stabilizing interactions between the two different cytoskeletal systems. The finding that *Drosophila* myosin VI binds directly to and largely co-localizes with a microtubule-binding protein, D-CLIP-190 [24] is also consistent with this mode of myosin VI action. *In vitro* analysis of spermatid budding by both the wild-type and mutant spermatocytes and localization of myosin VI throughout spermatogenesis, should allow us to establish more conclusively the role of this myosin.

On the basis of mutant analyses in mice and *Drosophila*, myosin VI has been suggested to play a part in moving membranes along actin filaments [9,10]. The mouse myosin VI mutant *Snell's waltzer* (*sv*) exhibits deafness and vestibular disorders [25]. The stereocilia of the inner and outer cochlear hair cells, actin-containing surface projections necessary for mechanosensation, are present but begin to degenerate soon after birth [26]. As the *sv* mice age, the membranes at the bases of stereocilia appear to fuse, suggesting that myosin VI may have a role in pulling membrane down along actin filaments [26]. Myosin VI germline mutations in *Drosophila* cause spermatogenesis defects as a result of failure of sperm separation during the process of individualization [27]. The *Drosophila* myosin VI is thought to have a role in delivering membrane vesicles to the leading edge of the advancing investment cones that pull membrane along the sperm and exclude unnecessary cellular components to the base of the sperm cyst, a waste-bag structure analogous to the RB [27]. Clearly, the morphological changes involved in spermatogenesis are different in *Drosophila* and *C. elegans*, and are reflected in the sperm that are formed: *Drosophila* sperm are flagellated whereas nematode sperm are not and, instead, exhibit amoeboid motility. It is intriguing that such seemingly different processes may share a common molecular mechanism involving myosin VI function. Continued study of the role of myosin VI in *C. elegans* spermatogenesis may provide further insight into the role of this motor protein in other cell types such as hair cells.

Conclusions

Deletion of a *C. elegans* class VI myosin results in a specific defect in spermatogenesis. Analysis of the mutant phenotype reveals that this motor protein has a role in the asymmetric partitioning of organelles and cytoskeletal elements during spermatogenesis.

Materials and methods

Nematode strains

Caenorhabditis elegans propagation and genetic manipulations were performed essentially as described [28]. The following strains were obtained from the *C. elegans* Genetics Center: N2. KR278 *hDf7 dpy-5(e61) unc-13(e450) I*; *sDp2 (I; f)*. BA785 *spe-8(hc40) I*. BA794 *spe-13(hc137) I*; SL3 *spe-15(hc75) I*; MT3100 *unc*-35*(n1338) I*; CB251 *unc-36(e251) III* . DR466 *him-5(e1490) V*. Two partly characterized Spe mutants originally isolated in the Schedl lab, *eb10* and *eb56*, which map near *spe-15* genetically, were obtained from a collection maintained by S.L'H.

Isolation of a hum-3 *deletion mutant*

A population of wild-type animals was mutagenized with trimethyl psoralen and ultraviolet light, split into pools and screened for deletions within *hum-3* (F47G6.4). Deletions were detected using PCR using nested sets of oligonucleotide primers. Further details of the screening procedure are available at http://snmc01.omrf.uokhsc.edu/revgen/RevGen.html. Outside primer sequences were external left 1 (EL1) 5′-CCGTTTTTCTCCCTGCATAA-3′ and external right 1 (ER1) 5′-TCTCGTCTCATAGCACACCG-3′. Inside primers were internal left 1 (IL1) 5′-ACATAGTACCGCGGATTTCG-3′ and internal right 1 (IR1) 5'-CATCCAATCGGAAGTGGTTC-3′. These primers span sequences encoding the core of the myosin VI motor domain.

spe-15(ok153) mutants were outcrossed eight times, using PCR to identify mutant animals. DNA spanning the *ok153* breakpoints was amplified by PCR and sequenced in the Microchemical Facility at the University of Minnesota using primers EL1 and ER1. During initial characterization, *hum-3(ok153)* was maintained *in trans* to *unc-35*. For maintenance and analysis of homozygous animals, *ok153* was placed *in cis* to *dpy-5* and balanced over the free duplication *sDp2* [29] in a *him-5* background.

Fertility tests

Hermaphrodite fertility was tested by picking single F1 hermaphrodite progeny from selfed *spe-15(ok153)/+* hermaphrodite F0 animals to individual seeded plates for three days to lay eggs, then removing the F1 animals to determine the genotype. F2 broods of *spe-15*(*ok153*) homozygotes were counted on day 4.

The ability of wild-type sperm to rescue *spe-15*(*ok153*) hermaphrodite self-sterility was tested by placing single *spe-15*(*ok153*) mutant hermaphrodites on seeded plates with 10 N2 males for 3 to 4 days. The number of progeny was scored on the fourth and fifth days.

Male fertility was tested as follows: *spe-15*(*ok153*)/+ males were crossed to *spe-15*(*ok153*) hermaphrodites to generate *spe-15*(*ok153*)/+ and *spe-15*(*ok153*) males. Single tester males were placed on 3 cm plates with three *unc-35* hermaphrodites and allowed to mate for 3 days before genotyping the male by PCR. Mating plates were scored on days 4 and 5 for non-Unc progeny.

Complementation testing

hum-3(ok153), approximate map position –15.42 on chromosome I, was tested for complementation of *spe-8* (–18.42), *spe-13* (–21.31) and *spe-15* (–16.23) as follows: *hum-3(ok153)*/+ males were crossed to *spe-8*, *spe-13* or *spe-15* hermaphrodites. Single hermaphrodite F1 progeny from these crosses were picked to individual plates and allowed to lay eggs (or oocytes) for 2 days before removing the F1 animals for PCR determination of the genotype. The presence or absence of F2 progeny was scored on the third, fourth and fifth days. Alternatively, *hum-3*(*ok153*) *dpy-5* hermaphrodites were crossed to *spe-8* males or *spe-13*/+ males and non-Dpy progeny were scored for fertility.

Molecular methods

spe-15(*hc75*) was sequenced as follows: the Expand High Fidelity PCR kit (Boehringer Mannheim) was used with custom oligonucleotide primers to amplify approximately 1 kb overlapping fragments encompassing all exons and intron–exon junctions within *hum-3*, using genomic DNA isolated from homozygous *spe-15* animals as template. All fragments were sequenced and contigs were assembled in SeqMan (DNASTAR). Candidate mutations were sequenced on both strands from two independent PCR amplifications.

Analysis of sperm

Spermatocytes and spermatids were dissected from age-matched marked, balanced *spe-15(ok153)* males or from an isogenic strain (defined as wild-type for these experiments) and analyzed in parallel. Dissections were performed in sperm media [21] containing 10 mM glucose (SMG) [30] by cutting through the tail at the vas deferens. To assay sperm activation *in vitro*, L4 males were picked to plates without hermaphrodites, grown for 10–12 h and dissected in SMG in the presence of 0.2 mg/ml pronase [31]. The number of activated spermatids was counted after 20 min. Spermatids and spermatocytes were fixed for fluorescent labeling in 2% formaldehyde and 0.25% picric acid [32] in SMG, pH 7.5. Mitochondria were labeled with anti-human COX1 monoclonal antibody (Molecular Probes) and MOs were labeled with monoclonal antibody 1CB4 [33] or with fluorescently conjugated wheat-germ agglutinin [31] (Molecular Probes), that gave staining coincident to 1CB4 (data not shown). Actin filaments were visualized with Alexa-568 phalloidin (Molecular Probes) in fixed cells. Tubulin was visualized by staining with anti-α-tubulin monoclonal antibody B-5-1-2 (Sigma). DNA was visualized with Hoechst 33342 (Sigma). Cells were observed with a Zeiss Axiovert equipped with DIC optics and images captured with either a CCD (DAGE-MTI CCD-100) or SpotRT digital (Diagnostic Instruments) camera controlled by Metamorph 4.5 software (Universal Imaging Corporation).

Acknowledgements

We thank Ann Rougvie, Mary Porter and Richard Tuxworth (UMN) for many helpful comments on the manuscript and the Twin Cities worm community for helpful discussions throughout the course of this work and for sharing reagents and expertise. J.F.K. thanks Ann Rougvie and members of her lab for providing lab space and training during the early part of this project. We would also like to thank Guang-dan Zhu (Emory University) for sharing his *eb10* and *eb56* complementation data. This work was supported by grants to J.F.K. (F32-GM19481), R.B. (HG01843), and S.W..L (GM40697), from the National Institutes of Health, a travel grant to J.F.K. from the National Science Foundation training grant for Interdisciplinary Studies on the Cytoskeleton (DIR9113444) at the University of Minnesota, and by an American Heart Association Established Investigator award (9940038N) to M.A.T. A number of strains used for this work were obtained from the *Caenorhabditis* Genetics Center at the University of Minnesota (St Paul), which is supported by a grant from the National Institutes of Health National Center for Research Resources.

References

1. Bobola N, Jansen RP, Shin TH, Nasmyth K: Asymmetric accumulation of Ash1p in postanaphase nuclei depends on a myosin and restricts yeast mating-type switching to mother cells. *Cell* 1996, 84:699-709.
2. Takizawa PA, Sil A, Swedlow JR, Herskowitz I, Vale RD: Actin-dependent localization of an RNA encoding a cell-fate determinant in yeast. *Nature* 1997, 389:90-93.
3. Bertrand E, Chartrand P, Schaefer M, Shenoy SM, Singer RH, Long RM: Localization of ***ASH1*** mRNA particles in living yeast. *Mol Cell* 1998, 2:437-445.
4. Guo S, Kemphues KJ: A non-muscle myosin required for embryonic polarity in ***Caenorhabditis elegans***. *Nature* 1996, 382:455-458.
5. Lu B, Ackerman L, Jan LY, Jan YN: Modes of protein movement that lead to the asymmetric localization of Partner of Numb during ***Drosophila*** neuroblast division. *Mol Cell* 1999, 4:883-891.
6. Baker JP, Titus MA: Myosins: matching motors with functions. *Curr Opin Cell Biol* 1998, 10:80-86.
7. Mermall V, Post PL, Mooseker MS: Unconventional myosins in cell movement, membrane traffic, and signal transduction. *Science* 1998, 279:527-533.
8. Wells AL, Lin AW, Chen LQ, Safer D, Cain SM, Hasson T, *et al.*: Myosin VI is an actin-based motor that moves backwards. *Nature* 1999, 401:505-508.
9. Rodriguez OC, Cheney RE: A new direction for myosin. *Trends Cell Biol* 2000, 10:307-311.
10. Titus MA: Getting to the point with myosin VI. *Curr Biol* 2000, 10:R294-R297.
11. L'Hernault SW: Spermatogenesis. In: *C. elegans II*. Edited by Riddle DL, Blumenthal T, Meyer BJ, Priess JR. Plainview, NY: Cold Spring Harbor Laboratory Press; 1997:271-294.
12. Varkey JP, Muhlrad PJ, Minniti AN, Dao B, Ward S: The ***Caenorhabditis elegans spe-26*** gene is necessary to form spermatids and encodes a protein similar to the actin-associated proteins kelch and scruin. *Genes Dev* 1995, 9:1074-1086.
13. Baker JP, Titus MA: A family of unconventional myosins from the nematode ***Caenorhabditis elegans***. *J Mol Biol* 1997, 272:523-535.

14. L'Hernault SW, Shakes DC, Ward S: Developmental genetics of chromosome I spermatogenesis-defective mutants in the nematode ***Caenorhabditis elegans***. *Genetics* 1988, 120:435-452.
15. Ward S, Argon Y, Nelson GA: Sperm morphogenesis in wild-type and fertilization defective mutants of ***Caenorhabditis elegans***. *J Cell Biol* 1981, 91:26-44.
16. Nelson GA, Roberts TM, Ward S: ***Caenorhabditis elegans*** spermatozoan locomotion: amoeboid movement with almost no actin. *J Cell Biol* 1982, 92:121-131.
17. Shakes DC, Ward S: Mutations that disrupt the morphogenesis and localization of a sperm-specific organelle in ***Caenorhabditis elegans***. *Dev Biol* 1989, 134:307-316.
18. Mahaca K, L'Hernault SW: The ***Caenorhabditis elegans spe-5*** gene is required for morphogenesis of a sperm-specific organelle and is associated with an inherent cold-sensitive phenotype. *Genetics* 1997, 146:567-581.
19. Ward S: Asymmetric localization of gene products during the development of ***Caenorhabditis elegans*** spermatozoa. In: *Gametogenesis and the Early Embryo*. Edited by Gall JG. New York: Alan R. Liss; 1986:55-75.
20. Arduengo PM, Appleberry OK, Chuang P, L'Hernault SW: The presenilin protein family member SPE-4 localizes to an ER/Golgi derived organelle and is required for proper cytoplasmic partitioning during ***Caenorhabditis elegans*** spermatogenesis. *J Cell Sci* 1998, 111:3645-3654.
21. L'Hernault SW, Roberts TM: Cell biology of nematode sperm. In: Caenorhabditis elegans*: Modern Biological Analysis of an Organism*. Edited by Epstein HF, Shakes DC. New York: Academic Press; 1995:273-301.
22. Roberts TM, Pavalko FM, Ward S: Membrane and cytoplasmic proteins are transported in the same organelle complex during nematode spermatogenesis. *J Cell Biol* 1986, 102:1787-1796.
23. Shakes DC, Ward S: Initiation of spermiogenesis in ***C. elegans***: a pharmacological and genetic analysis. *Dev Biol* 1989, 134:189-200.
24. Lantz VA, Miller KG: A class VI unconventional myosin is associated with a homologue of a microtubule-binding protein, cytoplasmic linker protein-170, in neurons and at the posterior pole of ***Drosophila*** embryos. *J Cell Biol* 1998, 140:897-910.
25. Avraham KB, Hasson T, Steel KP, Kingsley DM, Russell LB, Mooseker MS, Copeland NG, Jenkins NA: The mouse ***Snell's waltzer*** deafness gene encodes an unconventional myosin required for structural integrity of inner ear hair cells. *Nat Genet* 1995, 11:369-375.
26. Self T, Sobe T, Copeland NG, Jenkins NA, Avraham KB, Steel KP: Role of myosin VI in the differentiation of cochlear hair cells. *Dev Biol* 1999, 214:331-341.
27. Hicks JL, Deng WM, Rogat AD, Miller KG, Bownes M: Class VI unconventional myosin is required for spermatogenesis in ***Drosophila***. *Mol Biol Cell* 1999, 10:4341-4353.
28. Brenner S: The genetics of ***Caenorhabditis elegans***. *Genetics* 1974, 77:71-94.
29. Howell AM, Gilmour SG, Mancebo RA, Rose AM: Genetic analysis of a large autosomal region in ***C. elegans*** by the use of a free duplication. *Genet Res* 1987, 49:207-213.
30. Mahaca K, De Felice LJ, L'Hernault SW: A novel chloride channel localizes to ***Caenorhabditis elegans*** spermatids and chloride channel blockers induce spermatid differentiation. *Dev Biol* 1996, 176:1-16.
31. Ward S, Hogan E, Nelson GA: The initiation of spermiogenesis in the nematode ***Caenorhabditis elegans***. *Dev Biol* 1983, 98:70-79.
32. Humbel BM, Biegelmann E: A preparation protocol for postembedding immunoelectron microscopy of ***Dictyostelium discoideum*** cells with monoclonal antibodies. *Scan Microsc* 1992, 6:817-825.
33. Okamoto H, Thomson JN: Monoclonal antibodies which distinguish certain classes of neuronal and support cells in the nervous tissue of the nematode ***C. elegans***. *J Neurosci* 1985, 5:643-653.

Because *Current Biology* operates a 'Continuous Publication System' for Research Papers, this paper has been published on the internet before being printed. The paper can be accessed from http://biomednet.com/cbiology/cub